

## Scientific Report 04-09

### Comparison of vertical refractivity and temperature profiles from CHAMP with radiosonde measurements

Jens Wickert



## **Colophone**

**Serial title:**

Scientific Report 04-09

**Title:**

Comparison of vertical refractivity and temperature profiles from CHAMP with radiosonde measurements

**Subtitle:**

**Authors:**

Jens Wickert

**Other Contributors:**

**Responsible Institution:**

Danish Meteorological Institute  
GeoForschungsZentrum Potsdam

**Language:**

English

**Keywords:**

**Url:**

[www.dmi.dk/dmi/sr04-09](http://www.dmi.dk/dmi/sr04-09)

**ISSN:**

1399-1949

**ISBN:**

87-7478-511-7

**Version:**

**Website:**

[www.dmi.dk](http://www.dmi.dk)

**Copyright:**

Danish Meteorological Institute  
GeoForschungsZentrum Potsdam  
B. Kuo (fig.2.1)



## Contents

Colophone . . . . .	2
<b>1 Introduction</b>	<b>4</b>
<b>2 The global radiosonde network</b>	<b>4</b>
<b>3 CHAMP radio occultation data</b>	<b>6</b>
<b>4 Comparison with radiosondes</b>	<b>7</b>
4.1 Data sets and how to compare . . . . .	7
4.2 Comparison results . . . . .	7
<b>5 Summary and conclusions</b>	<b>23</b>
<b>Acknowledgements</b>	<b>24</b>

# Comparison of vertical refractivity and temperature profiles from CHAMP with radiosonde measurements

Jens Wickert

GeoForschungsZentrum Potsdam

Department Geodesy and Remote Sensing

Tel. +49 331 2881758; Fax +49 331 2881732; e-mail: wickert@gfz-potsdam.de

GRAS SAF Visiting scientist, October 2004

Note: This report has also been published as GFZ Scientific technical report 04/19, December 2004

## 1 Introduction

Atmospheric profiling with the German CHAMP (CHALLENGING Minisatellite Payload, *Reigber et al.* [2005]) satellite was activated on February 11, 2001 [*Wickert et al.*, 2001b]. The experiment brought significant progress [*Hajj et al.*, 2004; *Kuo et al.*, 2004; *Wickert et al.*, 2004c] for the innovative GPS (Global Positioning System) radio occultation (RO) technique in relation to the pioneering GPS/MET (GPS/METEorology) mission [e.g. *Ware et al.*, 1996; *Kursinski et al.*, 1996, 1997; *Rocken et al.*, 1997]. The measurements from CHAMP were and are precondition for various applications in atmospheric/ionospheric research [e.g. *Jakowski et al.*, 2002; *Ratnam et al.*, 2004; *Wickert et al.*, 2004b; *Wang et al.*, 2004; *Kuo et al.*, 2005], weather forecast [e.g. *Healy et al.*, 2005] and climate change detection [e.g. *Schmidt et al.*, 2004; *Foelsche et al.*, 2005]. The data are also used to prepare processing systems and analysis centers for upcoming RO missions, as, e.g., COSMIC (Constellation Observing System for Meteorology, Ionosphere and Climate, *Rocken et al.* [2000]; *Kuo et al.* [2004]) or MetOp (Meteorology Operational, *Loiselet et al.* [2000]; *Larsen et al.* [2005]). This study deals with comparisons of CHAMP measurements (globally distributed vertical profiles of atmospheric refractivity and temperature) with data from the global radiosonde (RS) network. Several aspects are investigated as, e.g., the dependence of the comparison results on the geographical region (i.e., on the type of the used radiosonde) and on the maximum distance  $d$  and maximum time difference  $\Delta t$  between CHAMP and corresponding RS measurements.

## 2 The global radiosonde network

The global radiosonde network (see Fig. 2.1) is the backbone of the operational data provision for global weather forecasts and a key data source for climatological investigations [e.g. *Soden and Lanzante*, 1995; *Seidel et al.*, 2001].

Radiosondes provide data between the Earth's surface and  $\sim 30$  km altitude with average vertical resolution of about 50 m. Under good weather conditions altitudes up to 40 km can be reached. For the accuracy of the RS data (e.g., for Vaisala RS-80) the manufactures [*Vaisala*, 1991] give (laboratory conditions): pressure 0.5 hPa, temperature 0.2 K and relative humidity 2%. However,

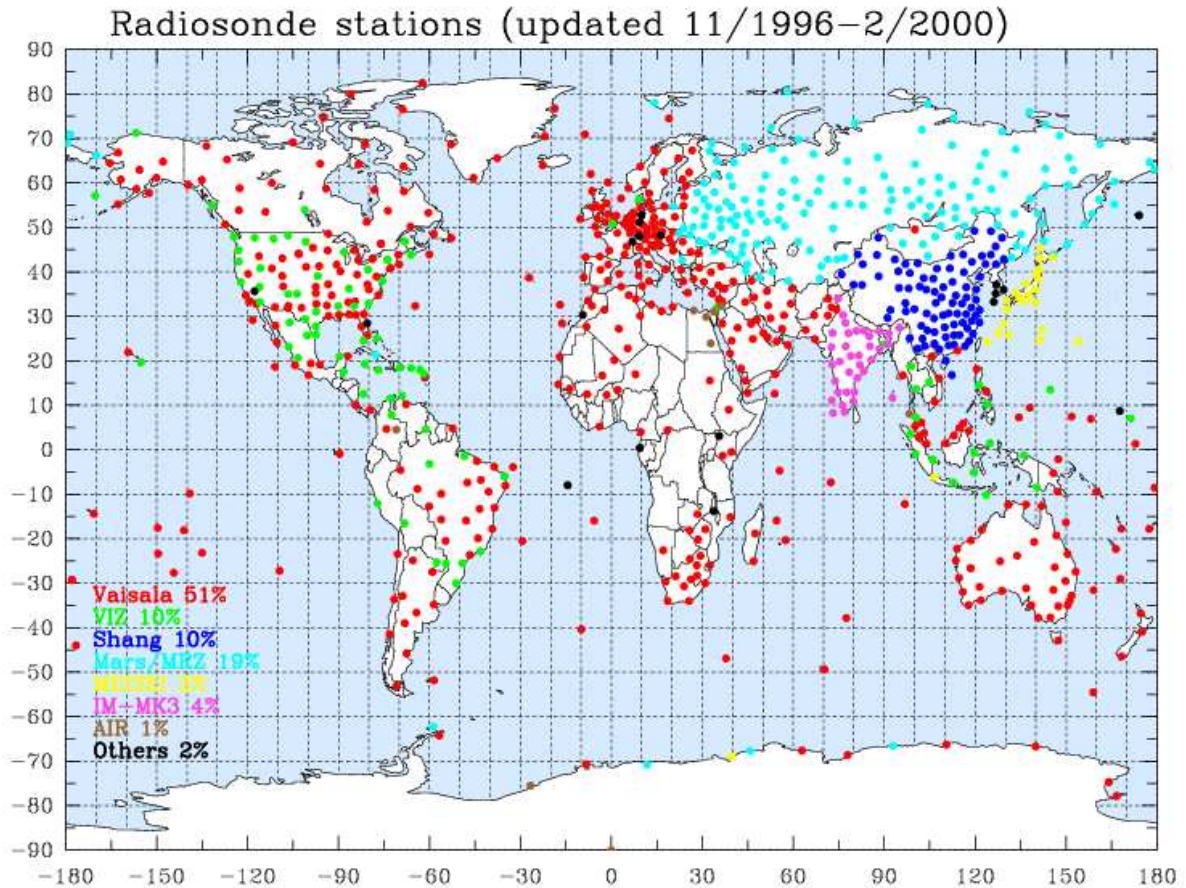


**Figure 2.1:** Geographical distribution of global radiosonde stations (total 852) colored by radiosonde types. The percentage given in the legend is the percentage of stations used by each type of radiosonde (from *Kuo et al.* [2005]).

due to radiation influence during the flight, actual accuracies may differ from these values. Because of errors in the determination of the pressure at higher altitudes and resulting incorrect assignment of the measurements to the altitude there can be temperature errors of  $\sim 1$  K above 10 km, and up to  $\sim 4$  K at 30 km [*Ware et al.*, 1996].

The humidity measurement of RS is a general problem. Particularly at low temperatures large errors (15% and more, *Dzingle and Leiterer* [1995]) are observed and some authors [e.g. *Elliot and Gaffen*, 1991] are in general doubt about the reliability (except in the Tropics) of humidity measurements from RS above 500 hPa (5-6 km altitude). A major problem of the humidity sensors is icing, when the sonde flies through clouds at temperatures below the freezing point of water. Improvements of the RS humidity measurements are recently achieved by using appropriate calibration schemes and twin humidity sensor configurations [*Leiterer et al.*, 1997].

Data from the global radiosonde network, as provided for the Global Telecommunication System (GTS) of the World Meteorological Organization (WMO), are used for the comparison with the CHAMP measurements. They were provided via the stratospheric research group at the Freie Universität Berlin. The WMO code (station identifier) was used to distinguish between different types of radiosondes [*Deutscher Wetterdienst*, 1996]. In a recent study from *Kuo et al.* [2005] it was found that the quality of the RS soundings over different geographical areas exhibit significant

variations. This was demonstrated by comparison with GPS RO data from CHAMP. According to this study Vaisala (Australia, Europe) and Shanghai (China) radiosondes show best agreement with GPS RO, largest differences are observed for IM-MK3 (India).

### 3 CHAMP radio occultation data

Analysis results (version 005) from the operational CHAMP occultation processing at GFZ are used for this study. Details of the analysis and processing system as well as recent validation results are given by, e.g., *Wickert et al.* [2004c]; *Beyerle et al.* [2005]; *Schmidt et al.* [2005]; *Wickert et al.* [2005a, b].

CHAMP data are analyzed using the standard double difference method to eliminate satellite clock errors [*Wickert et al.*, 2001a]. Atmospheric bending angles are derived from the time derivative of the excess phase after appropriate filtering. The ionospheric correction is performed by linear combination of the L1 and L2 bending angle profiles [*Vorob'ev and Krasil'nikova*, 1994]. The bending angles are optimized using the MSIS-90E atmospheric model [*Hedin*, 1991] applying the approach by *Sokolovskiy and Hunt* [1996]. To correct for the effect of lower troposphere multipath below 15 km the Full Spectrum Inversion (FSI) technique, a wave optics based analysis method, is applied [*Jensen et al.*, 2003].

Vertical profiles of atmospheric refractivity are derived from the ionosphere corrected bending angle profiles by Abel inversion. For dry air, the density profiles are obtained from the relationship between density and refractivity. Pressure and temperature (“dry temperature”) are obtained from the hydrostatic equation and the equation of state for an ideal gas. The temperature is initialized using ECMWF data (European Centre for Medium-Range Weather Forecasts) at 43 km. More details on the retrieval are given by *Wickert et al.* [2004c]. Basics of the GPS radio occultation technique and the derivation of atmospheric parameters are described, e.g., by *Kursinski et al.* [1997] or *Hajj et al.* [2002]. The refractivity and dry temperature profiles (Data product: CH-AI-3-ATM) are provided via the CHAMP data center at GFZ (<http://isdc.gfz-potsdam.de/champ>). An overview of all available occultation data and analysis results is given in Tab. 3.1.

Data	Explanation
CH-AI-1-HR	Occultation measurements from CHAMP (L1 & L2; 50Hz)
CH-AI-1-FID	Fiducial network data (P1, P2, L1, L2; 1Hz)
CH-AI-2-TAB	List of daily occultation events
CH-AI-2-PD*	Calibrated atmospheric excess phase for each occultation event
CH-AI-3-ATM	Vertical atmospheric profile (refractivity and dry temperature)
CH-AI-3-WVP*	Water vapor profile
CH-AI-3-TCR	Relative TEC data
CH-AI-3-IVP	Electron density profiles
CH-OG-3-RSO	Rapid Science Orbit data of CHAMP and the GPS satellites

**Table 3.1:** Overview of available GPS occultation data and analysis results at the CHAMP data center (ISDC) of GFZ Potsdam <http://isdc.gfz-potsdam.de/champ>. \*The atmospheric excess phase and water vapor data are not routinely made available by the data center. Both types of analysis results are provided on demand. TCR and IVP products are generated by DLR Neustrelitz [see, e.g., *Jakowski et al.*, 2002].

## 4 Comparison with radiosondes

### 4.1 Data sets and how to compare

CHAMP data between May 15, 2001 and September 6, 2004 are used for the comparisons. 162,461 vertical profiles of refractivity and dry temperature (Data product CH-AI-3-ATM, Version 005, see Chap. 3) are available at the GFZ data center (<http://isdc.gfz-potsdam.de/champ>) for this period. Temperatures and refractivities are compared at the 19 main pressure levels  $l$  of the RS data files: 1000, 900, 800, 700, 600, 500, 400, 300, 200, 100, 90, 80, 70, 60, 50, 40, 30, 20, and 10 hPa. The refractivity from the RS data was calculated according to Eqn. 4.1 [Smith and Weintraub, 1953] with  $p$  atmospheric pressure and  $p_w$  water vapor partial pressure in hPa and temperature  $T$  in K. The saturation pressure over water is used to calculate  $p_w$  from the relative humidity, which is given in the RS data files, according to the definition in meteorological schoolbooks [e.g., Kraus, 2001].

$$N = 77.6 \frac{p}{T} + 3.73 \times 10^5 \frac{p_w}{T^2}. \quad (4.1)$$

The mean temperature deviation at each pressure level  $\overline{\Delta T(l)}$  and its standard deviation  $\sigma_{\Delta T(l)}$  was calculated according to Eqns. 4.2 and 4.3.  $M(l)$  denotes the number of data points at each pressure level. The index  $i$  indicates the individual pairs of coinciding CHAMP and RS data.  $T_{D(CHAMP)}$  is the dry temperature, derived from the CHAMP data (see Chap. 3).

$$\overline{\Delta T(l)} = \sum_{i=1}^{M(l)} T_{D(CHAMP)}(i, l) - T_{RS}(i, l). \quad (4.2)$$

$$\sigma_{\Delta T(l)} = \sqrt{\frac{1}{M(l) - 1} \sum_{i=1}^{M(l)} (T_{D(CHAMP)}(i, l) - T_{RS}(i, l))^2}. \quad (4.3)$$

The mean relative refractivity deviation at each pressure level  $\overline{\Delta N(l)}$  and its standard deviation  $\sigma_{\Delta N(l)}$  was calculated according to Eqns. 4.4 and 4.5.

$$\overline{\Delta N(l)} = \sum_{i=1}^{M(l)} \frac{N_{CHAMP}(i, l) - N_{RS}(i, l)}{N_{RS}(i, l)}. \quad (4.4)$$

$$\sigma_{\Delta N(l)} = \sqrt{\frac{1}{M(l) - 1} \sum_{i=1}^{M(l)} \left( \frac{N_{CHAMP}(i, l) - N_{RS}(i, l)}{N_{RS}(i, l)} \right)^2}. \quad (4.5)$$

The CHAMP data (version 005), provided via the GFZ data center, are quality checked. The maximum deviation of the refractivity values in relation to ECMWF is 10 %. To eliminate the disadvantageous influence of outliers in the RS data to the comparisons, similar criteria are applied. Data pairs are excluded, which exhibit more than 20 K deviation (temperature) and 10 % deviation (refractivity), respectively.

## 4.2 Comparison results

### 4.2.1 CHAMP vs. RS over Europe

The European region (WMO station code <20000; Vaisala radiosondes) was used to investigate the influence of the maximum time difference  $\Delta t$  and maximum radial distance  $d$  between CHAMP and RS measurement on the comparison results.  $\Delta t$  was varied between 1 and 3 h,  $d$  between 100 and 300 km.

The results of the comparisons are shown in Figs. 4.1-4.9. The combinations of  $\Delta t$  and  $d$  and the corresponding number of CHAMP/RS coincidences are summarized in Tab. 4.1. This table also shows the biases and standard deviations of the refractivity at the 100 hPa pressure level (in the vertical region of highest accuracy of GPS RO data, see, e.g., *Kursinski et al.* [1997]).

The resulting refractivity bias is practically independent of the used combination of  $d$  and  $\Delta t$ . The standard deviation is lowest for  $d = 100 \text{ km}$  with  $\sim 0.5\%$  and increases to  $\sim 0.7\%$  for  $d = 300 \text{ km}$ . Therefore the variation of  $d$  is more significant to the comparison results, rather than variation of  $\Delta t$ . Because the bias between CHAMP and RS measurements is practically not influenced by the various combinations of  $d$  and  $\Delta t$ , a combination of  $d = 300 \text{ km}$  and  $\Delta t = 3 \text{ h}$  was chosen for the subsequent investigations to get more statistical confidence by using more extensive data sets.

Before the comparison results are discussed in more detail, it is noted, that the refractivity, derived from the GPS occultation measurements, is the more independent variable rather than the temperature. The refractivity can be retrieved without "background", i.e., additional meteorological information, e.g., from ECMWF. Additional assumptions must be made to derive the temperature (see Chap. 3). It is also noted, that dry temperatures  $T_D$  from CHAMP (see Chap. 3) are compared with the "wet" temperature  $T$  from the radiosondes.

In general Fig. 4.1-4.9 look quite similar. The refractivity (middle panel) shows nearly no bias between about 600 hPa ( $\sim 4 \text{ km}$ ) and 30 hPa ( $\sim 24 \text{ km}$ ). Above the 30 hPa level a positive bias up to 0.5 (e.g., Fig. 4.5) - 0.8 % (e.g., Fig. 4.3) at 10 hPa of the CHAMP refractivities in relation to the RS data is observed. This refractivity bias is combined with a cold bias of the CHAMP temperatures in relation to the RS data up to 2 (e.g., Fig. 4.5) - 2.5 K (e.g., Fig. 4.3) at 10 hPa.

$d$ [km]	$\Delta t$ [h]	Coincidences	$\Delta N(100 \text{ hPa})[\%]$	$\sigma_{\Delta N}(100 \text{ hPa})[\%]$
100	1	212	0.14	0.57
100	2	386	0.11	0.54
100	3	585	0.10	0.52
200	1	787	0.10	0.66
200	2	1536	0.12	0.66
200	3	2362	0.12	0.67
300	1	1627	0.11	0.70
300	2	3367	0.12	0.73
300	3	5153	0.14	0.74

**Table 4.1:** Number of coincidences between CHAMP RO measurements and radio soundings over Europe (May 2001-September 2004) and corresponding refractivity bias and RMS of CHAMP vs. RS at 100 hPa.  $\Delta t$  is the maximum time difference and  $d$  the maximum radial distance between the corresponding CHAMP and RS profiles.

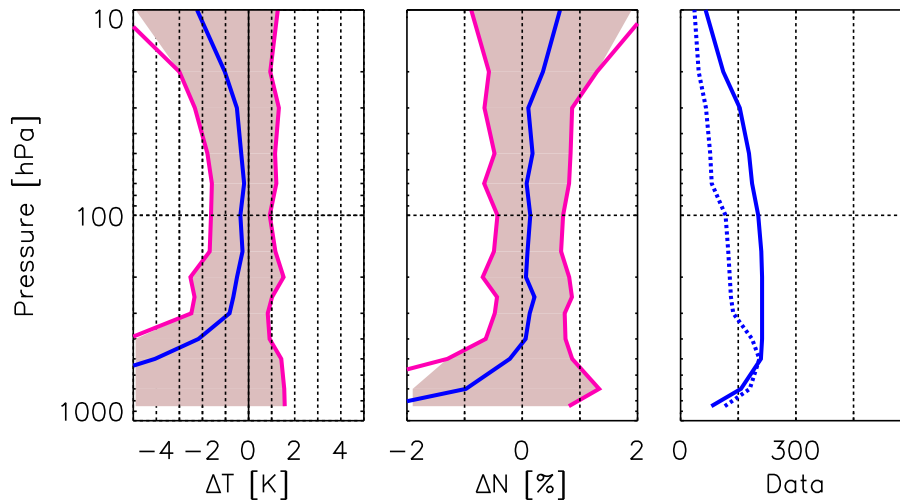


**Figure 4.1:** Comparison (Bias and RMS) of CHAMP dry temperature (left panel) and refractivity (middle) profiles with corresponding RS data (CHAMP-RS) over Europe for May 2001-September 2004 ( $\Delta t = 1 h$ ;  $d = 100 km$ ). The right panel shows the number of compared data per altitude (solid line: temperature; dashed line: refractivity).

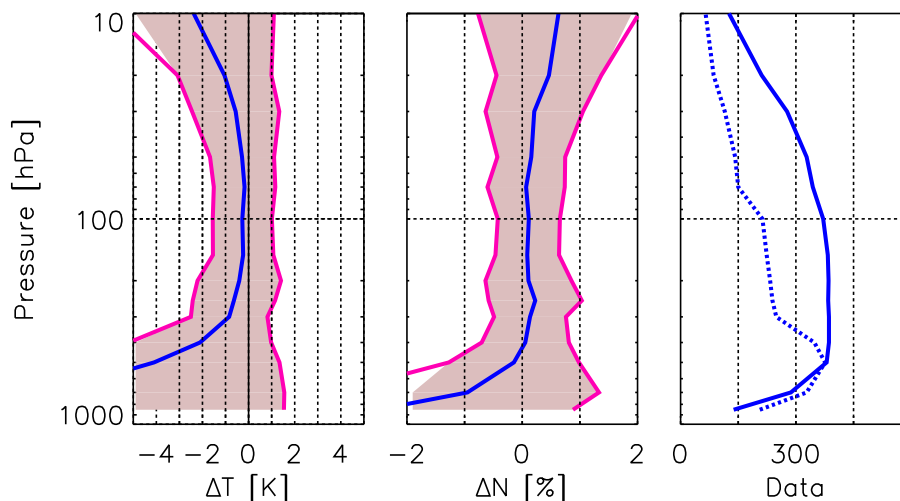


**Figure 4.2:** Comparison (Bias and RMS) of CHAMP dry temperature (left panel) and refractivity (middle) profiles with corresponding RS data (CHAMP-RS) over Europe for May 2001-October 2004 ( $\Delta t = 2 h$ ;  $d = 100 km$ ). The right panel shows the number of compared data per altitude (solid line: temperature; dashed line: refractivity).

The refractivity comparison in the lower troposphere is dominated by the appearance of a negative refractivity bias of the CHAMP measurements in relation to the RS data. This is a known feature from several CHAMP validation studies [e.g., Wickert, 2002; Marquardt et al., 2003; Kuo et al., 2004; Wickert et al., 2004a]. It is discussed in more detail by Ao et al. [2003]; Beyerle et al. [2003a, b, 2005]. Causes of the bias are, beside multi-path propagation, also signal tracking errors of the GPS receiver aboard CHAMP and critical refraction, a physical limitation of the RO technique. Further progress in reducing the bias is expected by the application of advanced signal tracking methods (Open Loop technique, see, e.g., [Sokolovskiy, 2001] or [Beyerle et al., 2005]) and improved signal strength due to the use of more advanced occultation antenna configuration (foreseen, e.g., for COSMIC or MetOp).

The lower troposphere refractivity bias is artificially enhanced here, when using the pressure as

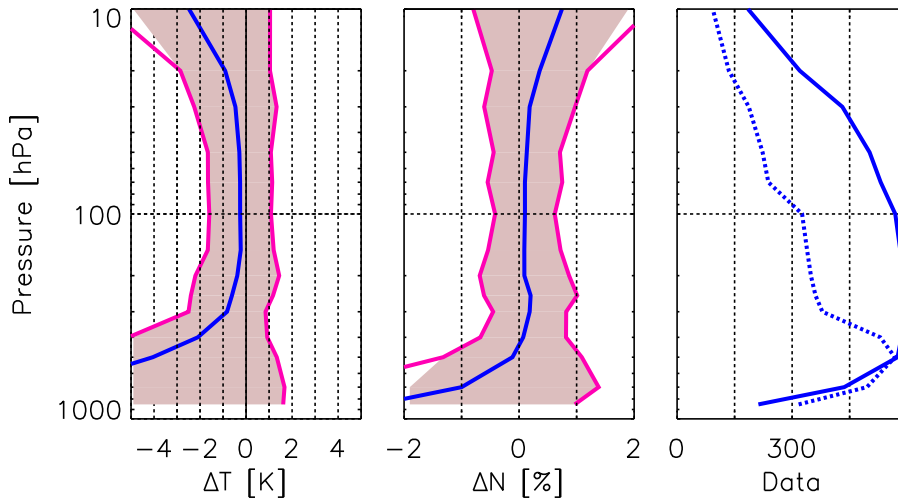


**Figure 4.3:** Comparison (Bias and RMS) of CHAMP dry temperature (left panel) and refractivity (middle) profiles with corresponding RS data (CHAMP-RS) over Europe for May 2001-September 2004 ( $\Delta t = 3 \text{ h}$ ;  $d = 100 \text{ km}$ ). The right panel shows the number of compared data per altitude (solid line: temperature; dashed line: refractivity).

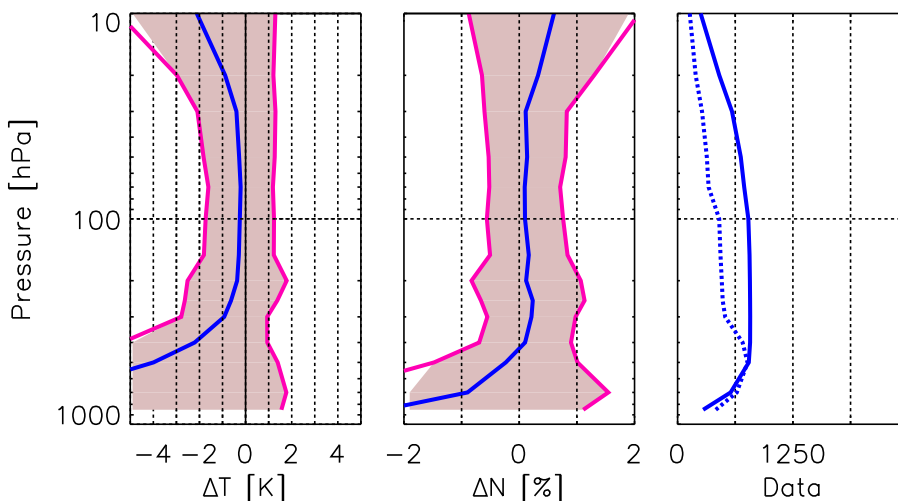


**Figure 4.4:** Comparison (Bias and RMS) of CHAMP dry temperature (left panel) and refractivity (middle) profiles with corresponding RS data (CHAMP-RS) over Europe for May 2001-September 2004 ( $\Delta t = 1 \text{ h}$ ;  $d = 200 \text{ km}$ ). The right panel shows the number of compared data per altitude (solid line: temperature; dashed line: refractivity).

altitude coordinate. Since the pressure is retrieved by integrating the air density (which is direct proportional to the refractivity in case of dry air) a smaller, as the real, pressure is calculated in the presence of "less than real" refractivity (i.e., the negative bias). Consequently the refractivity deviations are assigned to higher than the real altitudes, when a negative bias exist. Then, a larger bias as the real one is assigned to this height. This is the reason for the larger refractivity bias in the RS comparisons (pressure as altitude coordinate) compared to the Figs. 4.17-4.22, where the CHAMP data were compared with meteorological analyzes at geometrical altitudes.

A cold bias of the CHAMP dry temperature in relation to the RS data is obvious in Figs. 4.1-4.9. If water vapor is present, the dry air assumption for the derivation of the temperature (see Chap. 3) is not valid. It can be concluded from Eqn. 4.1 that temperature (dry temperature), derived assuming dry air assumption must be colder than the real temperature in the presence of water vapor as it can

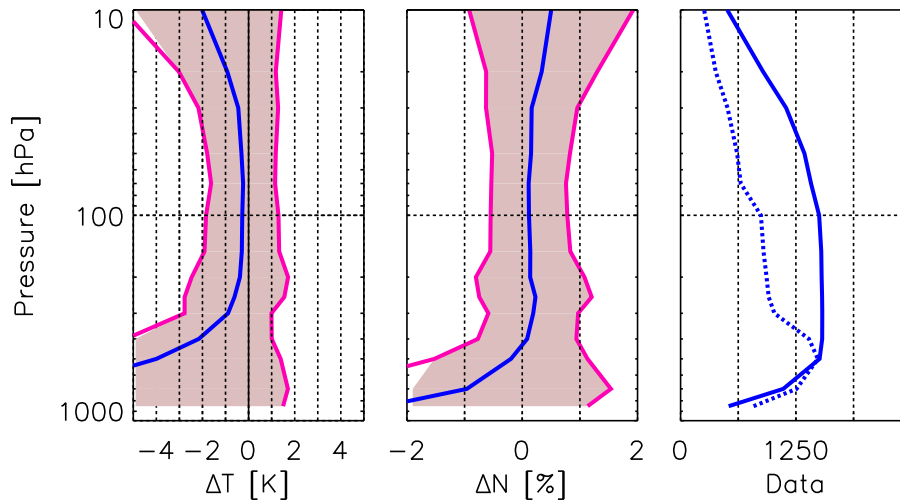


**Figure 4.5:** Comparison (Bias and RMS) of CHAMP dry temperature (left panel) and refractivity (middle) profiles with corresponding RS data (CHAMP-RS) over Europe for May 2001-September 2004 ( $\Delta t = 2 h$ ;  $d = 200 km$ ). The right panel shows the number of compared data per altitude (solid line: temperature; dashed line: refractivity).

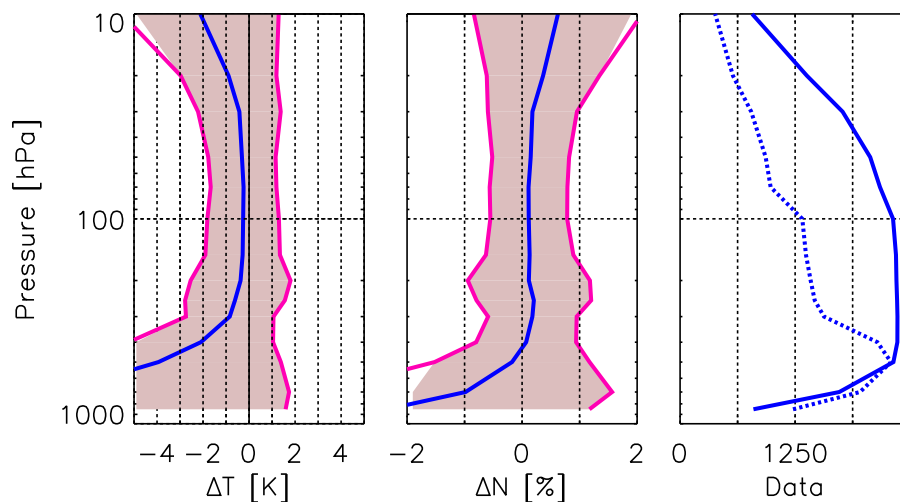


**Figure 4.6:** Comparison (Bias and RMS) of CHAMP dry temperature (left panel) and refractivity (middle) profiles with corresponding RS data (CHAMP-RS) over Europe for May 2001-September 2004 ( $\Delta t = 3 h$ ;  $d = 200 km$ ). The right panel shows the number of compared data per altitude (solid line: temperature; dashed line: refractivity).

be observed in Figs. 4.1-4.9. The deviation between both values is a measure for the water vapor partial pressure.

The onset of this dry temperature cold bias starts to be remarkable below  $\sim 9 km$ , i.e. the vertical region when water vapor is more and more present in the atmosphere. In contrast the refractivity is nearly bias-free in relation to the RS data down to 4-5 km. This proves the fact (assuming that the RS refractivity measurement is accurate in that altitude region) that the refractivity from GPS RO can be used for precise monitoring of the atmospheric state within that altitude interval, even in the presence of water vapor. Also RS data can be incorrect at these altitudes [e.g., *Leiterer et al.*, 1997].

The right panels of the Figs. 4.1-4.9 show the corresponding number of compared data per altitude. This number is decreasing with height, reflecting the fact, that most radiosondes do not reach the

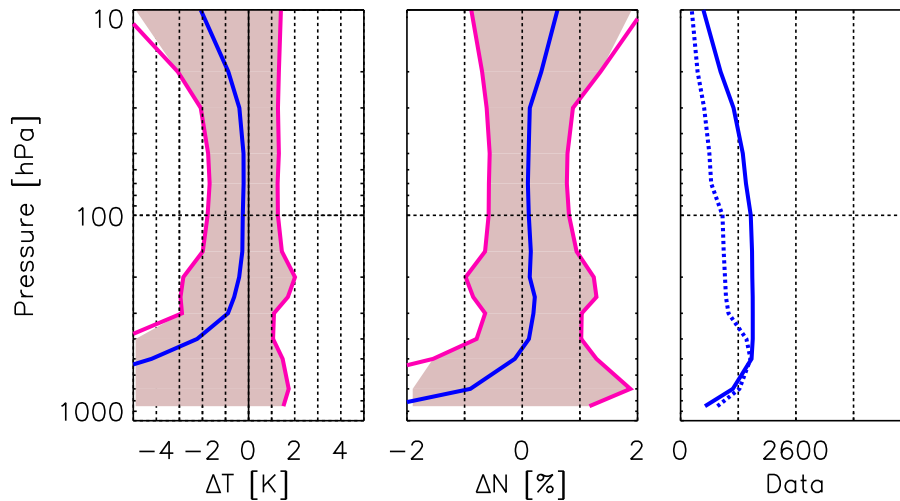


**Figure 4.7:** Comparison (Bias and RMS) of CHAMP dry temperature (left panel) and refractivity (middle) profiles with corresponding RS data (CHAMP-RS) over Europe for May 2001-September 2004 ( $\Delta t = 1 h$ ;  $d = 300 km$ ). The right panel shows the number of compared data per altitude (solid line: temperature; dashed line: refractivity).

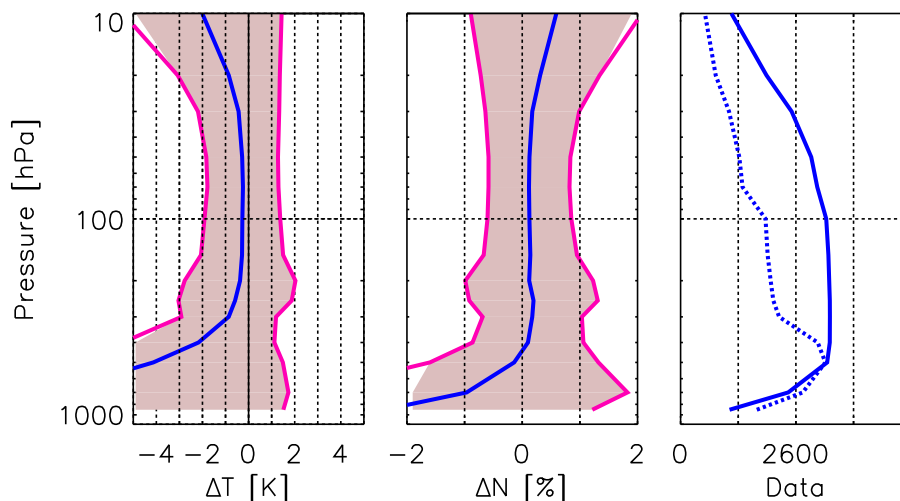


**Figure 4.8:** Comparison (Bias and RMS) of CHAMP dry temperature (left panel) and refractivity (middle) profiles with corresponding RS data (CHAMP-RS) over Europe for May 2001-September 2004 ( $\Delta t = 2 h$ ;  $d = 300 km$ ). The right panel shows the number of compared data per altitude (solid line: temperature; dashed line: refractivity).

10 hPa level. In the lower troposphere the situation is different. Here the number of GPS RO data, available per height, is decreasing with decreasing altitude. This is related to the known refractivity bias, which is discussed above. One consequence of, e.g., the tracking problems, is, that a significant percentage of the profiles does not reach the lowest part of the troposphere (excluding of lower troposphere data by the quality control parameter, derived from the FSI retrieval [Jensen *et al.*, 2003]).

The number of compared temperature data is larger than that of the corresponding refractivities, because the water vapor values, which are needed to calculate the refractivity values, were absent in the radiosonde data. Below the height of the onset of the negative GPS RO refractivity bias, there are slightly more refractivity data. This can be explained by the application of the quality criterion, which eliminates outliers (20 K deviation). In the presence of much water vapor (lower troposphere),

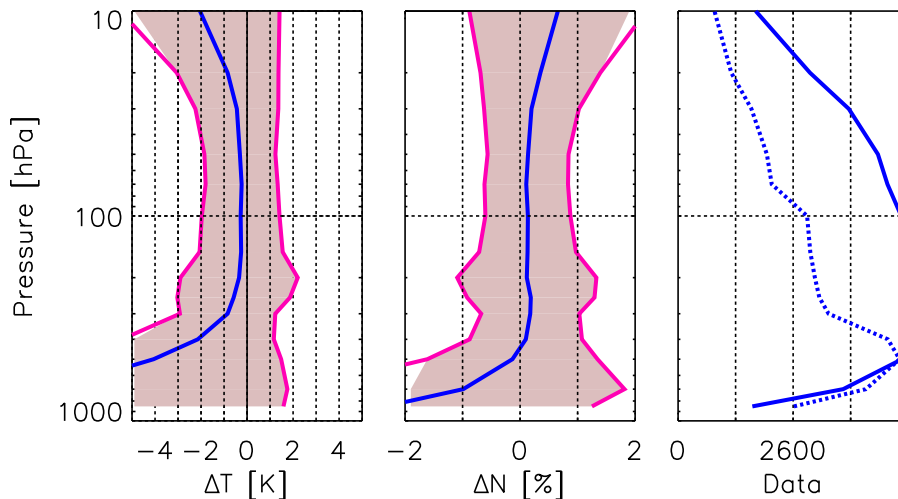


**Figure 4.9:** Comparison (Bias and RMS) of CHAMP dry temperature (left panel) and refractivity (middle) profiles with corresponding RS data (CHAMP-RS) over Europe for May 2001-September 2004 ( $\Delta t = 3 h$ ;  $d = 300 km$ ). The right panel shows the number of compared data per altitude (solid line: temperature; dashed line: refractivity).

the dry temperature from CHAMP may deviate from the RS temperatures by these values (see discussion above). The percentage of these profiles increases with decreasing altitude. This is reflected in Figs. 4.1-4.9.

#### 4.2.2 CHAMP vs. RS over other regions

Subsets of CHAMP data were generated to investigate the influence of different radiosonde types (according to various geographical regions) to the comparison results. The European region (predominant use of Vaisala RS) was already studied in more detail in Sec. 4.2.1. Here, the geographical regions Australia (WMO code 94120-94998), China (50000-60000), the countries of the former Soviet Union (SU, 20000-40000), India (41500-44000), Japan (47400-48000) and U.S. (70000-75000) are investigated. Over these regions the RS types Vaisala, Shanghai, Mars/MRZ, IM-MK3, Meisei and VIZ/Vaisala are used for the RS measurements (see Fig. 2.1). The results of the comparisons are shown in Figs. 4.10-4.15; a combination of  $d = 300 km$  and  $\Delta t = 3 h$  was used. For the U.S. region it is difficult to identify the type of the used RS if only the WMO code is used for identification. For the WMO code 70000-75000 there are predominantly two types of RS: VIZ and Vaisala. Nevertheless, for each of the other regions exist only one predominantly used RS type.

To verify, that the expected differences in the comparisons with the RS over the various geographical regions are not due to different meteorological conditions, the same data sets were also compared with ECMWF (see Chap. 4.2.3).

Tab. 4.2 overviews the data sets for the RS and ECMWF comparisons for different geographical regions. It is noted, that the number of the CHAMP data compared with ECMWF can be lower as for those with RS. In quite frequent cases more than one RS meets the CHAMP sounding, especially if there is a high area density of RS stations in the investigated geographical region, as, e.g., at Europe, China or U.S..

A problem of the RS data is their incomplete coverage of the altitude range up to 30 km due to balloon or sensor problems. E.g., it is often observed that humidity data for higher altitudes are not available (see also Tab. 4.3). However these data are required to calculate the refractivity from the

RS data (see Eqn. 4.1). Consequently the number of comparisons for the refractivity  $N$  and temperature  $T$  can be different. This is illustrated in the right panels of Figs. 4.10-4.15, where the number of compared data vs. altitude is plotted for the refractivity and temperature, respectively. It is noted, that the used data sets of temperature and refractivity may show slightly different statistical behavior while comparing with the RS data (the number of refractivity and temperature data is not the same; see the right panels of Figs. 4.10-4.15). This may lead to slight discrepancies, when the results of the refractivity and temperature comparison of each of the Figs. 4.10-4.15 are examined for consistency.

The vertical coverage with humidity data was worse for India and Japan (see Tab. 4.4). For that reason the relative humidity was set for these two data sets to 0 above altitudes equivalent to the 300 hPa level. The temperature at these heights is below  $\sim 40^\circ\text{C}$ , on first order the humidity then can be neglected due to the exponentially decreasing water vapor saturation pressure with altitude.

All data sets show the characteristic lower troposphere refractivity bias of the CHAMP data, which was discussed in detail already in Sec. 4.2.1. The comparison of the dry temperature from CHAMP with the RS temperature leads to a cold bias of the CHAMP in relation to the RS data when water vapor is present in the atmosphere. The magnitude of this bias is a measure for the water vapor content itself. This bias can be eliminated, if additional data are included to the retrieval to solve for the ambiguity of dry and wet term to the refractivity in Eqn. 4.1. Several methods are in use to derive temperature and water vapor profiles in the lower troposphere. One may assume the "background" temperature (e.g., ECMWF) as the truth and calculate water vapor profiles using iterative [e.g., *Gorbunov and Sokolovskiy, 1993*] or direct [e.g., *Heise et al., 2005*] methods. Temperature and water vapor also can be estimated applying 1Dvar techniques taking into account the error

Region	No. vs. RS	No. vs. ECMWF
Australia	813	756
China	2344	1186
Europe	5153	2946
Former SU	3093	2556
India	552	401
Japan	586	331
U.S.	5694	4372

**Table 4.2:** Number of profiles for the RS and ECMWF comparisons over different geographical regions ( $\Delta t = 3 h$ ;  $d = 300 km$ ).

Region	Prof.	100 hPa[%]	100 hPa <sub>WVP</sub> [%]	10 hPa[%]	10 hPa <sub>WVP</sub> [%]
Australia	813	98.03	13.78	18.45	16.48
China	2344	94.99	21.70	14.76	2.61
Europe	5153	97.88	56.59	34.06	15.97
Former SU	3093	87.50	74.58	10.78	8.41
India	552	56.52	0.18	0.36	0.00
Japan	586	100.00	0.00	65.01	0.00
U.S.	5694	97.17	95.99	72.84	71.39

**Table 4.3:** Data availability for RS profiles at the 100 and 10 hPa pressure levels depending on the investigated geographical region ( $\Delta t = 3 h$ ;  $d = 300 km$  in relation to CHAMP soundings).

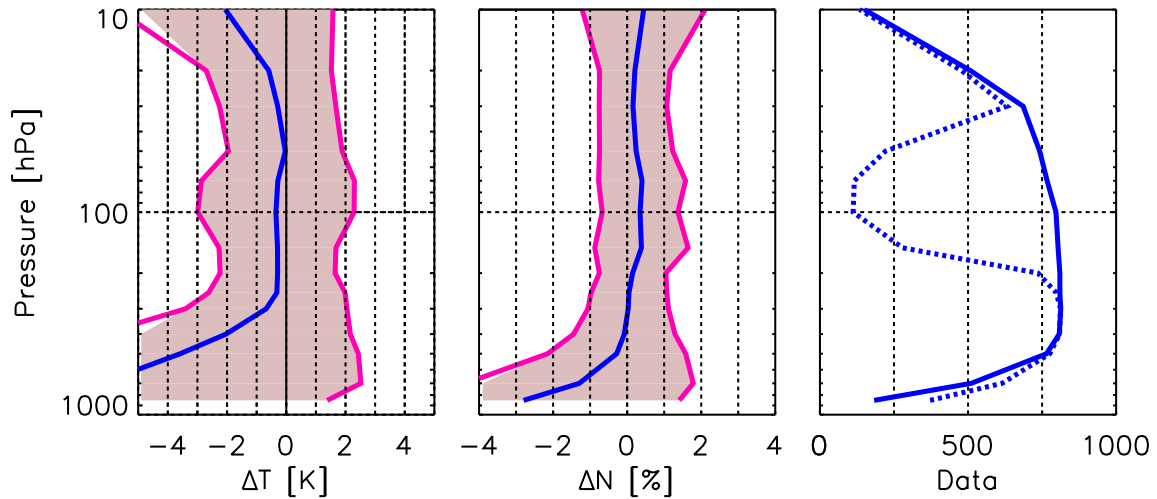


**Figure 4.10:** Comparison (Bias and RMS) of CHAMP dry temperature (left panel) and refractivity (middle) profiles with corresponding RS data (CHAMP-RS) over Australia for May 2001-September 2004 ( $\Delta t = 3 h$ ;  $d = 300 km$ ). The right panel shows the number of compared data per altitude (solid line: temperature; dashed line: refractivity).

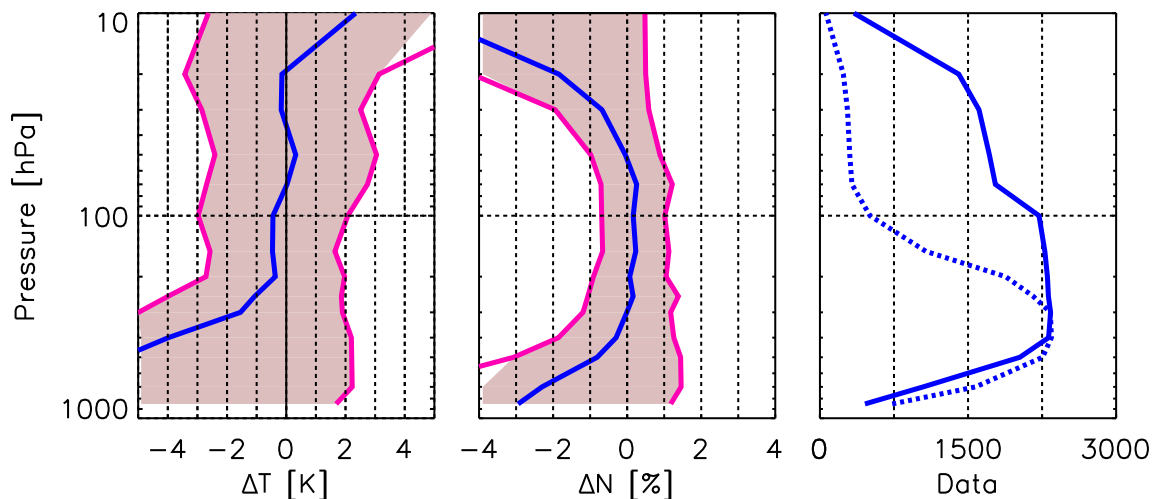


**Figure 4.11:** Comparison (Bias and RMS) of CHAMP dry temperature (left panel) and refractivity (middle) profiles with corresponding RS data (CHAMP-RS) over China for May 2001-September 2004 ( $\Delta t = 3 h$ ;  $d = 300 km$ ). The right panel shows the number of compared data per altitude (solid line: temperature; dashed line: refractivity).

characteristics of measurement and the background data [e.g., *Healy and Eyre, 2000*]. A problem of the 1Dvar techniques is non-satisfactorily knowledge of precise measurement and background (meteorological analyzes) errors. For that reason the wet-dry ambiguity was not solved for. The focus of this study are altitudes above 5-8 km, where the water vapor influence is small.

Best agreement of CHAMP and RS data is observed over Australia (Vaisala, Fig. 4.10), Europe (Vaisala, Fig. 4.9), Japan (Meisei, Fig. 4.14) and the U.S. (VIZ/Vaisala, Fig. 4.15). The refractivity of CHAMP is nearly bias free in relation to the RS data above  $\sim 500$  hPa up to 10 hPa for these regions. Standard deviations less than 1% at 100 hPa and  $\sim 1.5\%$  at 10 hPa are observed (see Tabs. 4.4 and 4.5). Hereby the comparison over the U.S. shows nearly perfect agreement (e.g., 0.03% at 100 hPa) for a set of nearly 6000 profiles; a remarkable result. It is noted that the CHAMP data are of highest accuracy in this vertical region [e.g., *Kursinski et al., 1997*]. Small biases are observed for

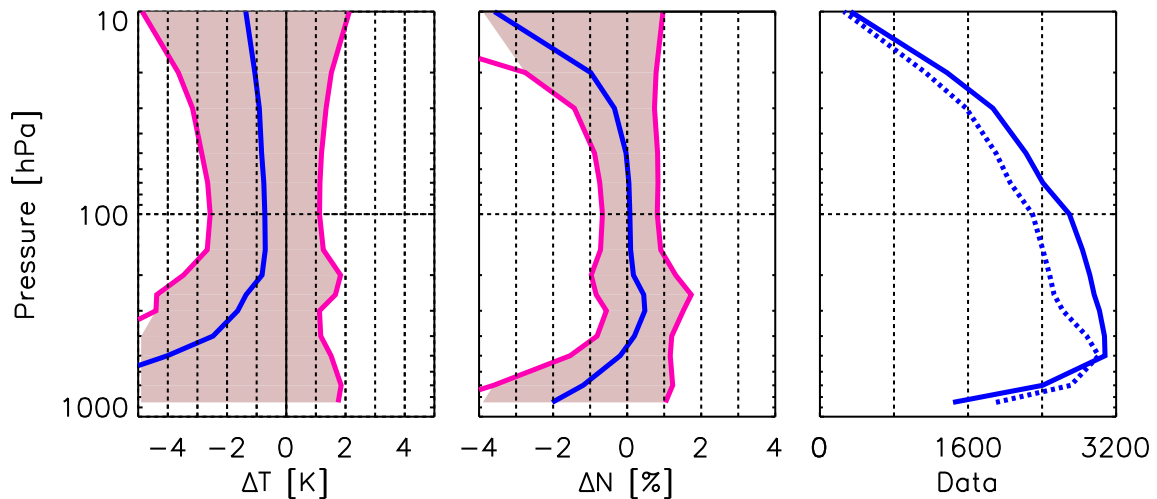


**Figure 4.12:** Comparison (Bias and RMS) of CHAMP dry temperature (left panel) and refractivity (middle) profiles with corresponding RS data (CHAMP-RS) over the countries of the former SU for May 2001-September 2004 ( $\Delta t = 3 h$ ;  $d = 300 km$ ). The right panel shows the number of compared data per altitude (solid line: temperature; dashed line: refractivity).

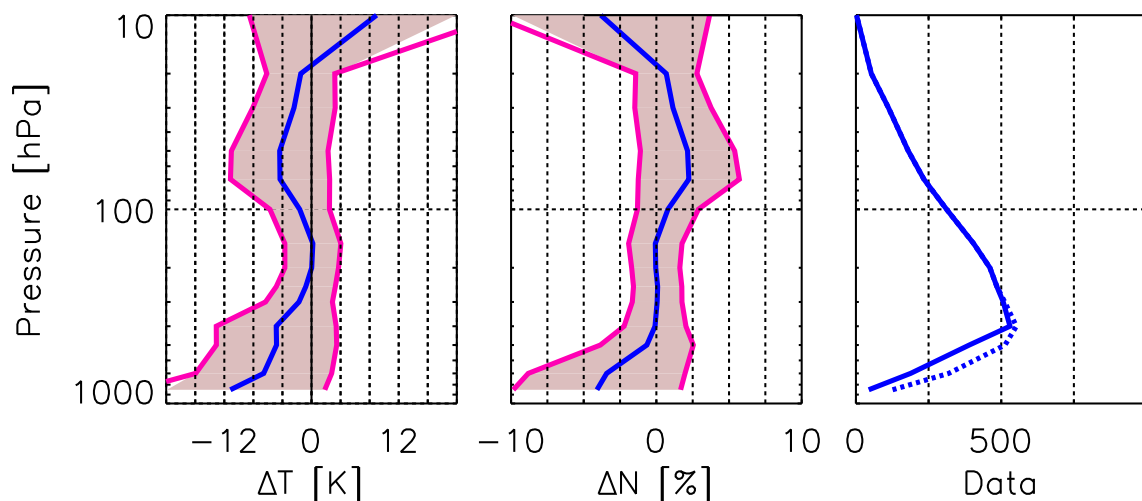


**Figure 4.13:** Comparison (Bias and RMS) of CHAMP dry temperature (left panel) and refractivity (middle) profiles with corresponding RS data (CHAMP-RS) over India for May 2001-September 2004 ( $\Delta t = 3 h$ ;  $d = 300 km$ ). The right panel shows the number of compared data per altitude (solid line: temperature; dashed line: refractivity).

Europe (0.13%), Australia (0.35%) and Japan (water vapor was set to 0 above 300 hPa; 0.22%). The major difference of the U.S. data set in relation to the others with good agreement is the nearly complete vertical coverage with water vapor data. The, in part, lack of them over the other regions is an indication of problems in the water vapor measurements of the RS at these altitudes, which may cause the small refractivity biases in relation to the CHAMP data. When biases are observed at 100 hPa (e.g., Australia or Europe) they are positive, i.e. CHAMP refractivities are slightly larger than the RS data. A reason for this can be an underestimation of the real water vapor values by the RS data (Vaisala for Europe and Australia).

For China (Shanghai sonde, Fig. 4.11) and the former SU (Mars/MRZ, Fig. 4.12) less perfect agreement is found. The main difference to the above discussed regions is the appearance of a large bias at higher altitudes (-3.58% former SU, -5.60% China at 10 hPa) which is connected with higher

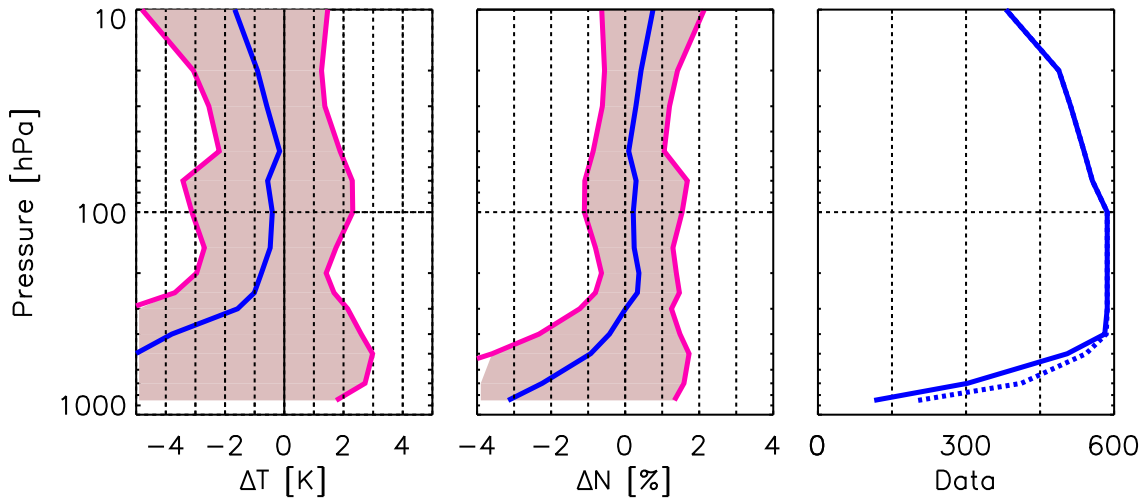


**Figure 4.14:** Comparison (Bias and RMS) of CHAMP dry temperature (left panel) and refractivity (middle) profiles with corresponding RS data (CHAMP-RS) over Japan for May 2001-September 2004 ( $\Delta t = 3 h$ ;  $d = 300 km$ ). The right panel shows the number of compared data per altitude (solid line: temperature; dashed line: refractivity).

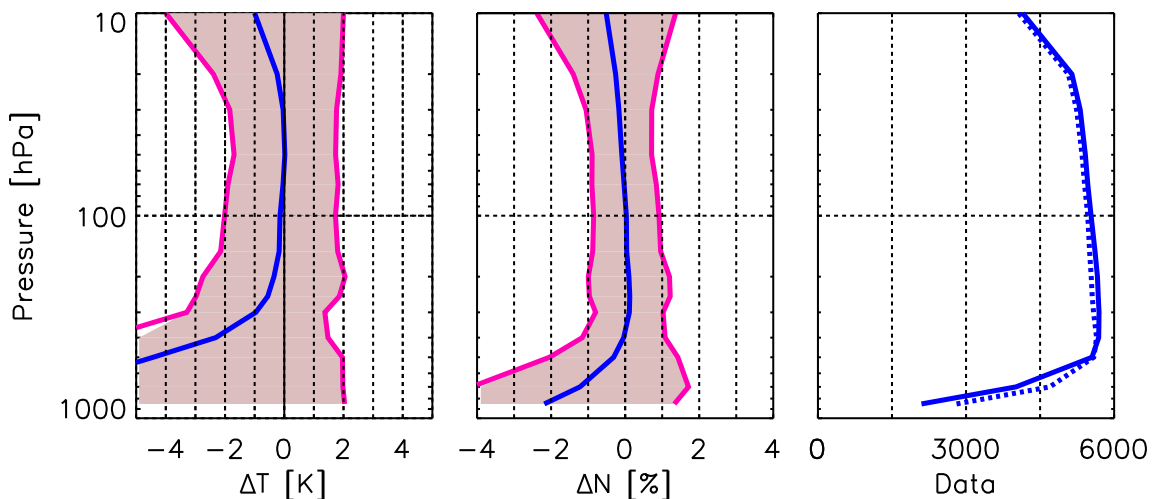


**Figure 4.15:** Comparison (Bias and RMS) of CHAMP dry temperature (left panel) and refractivity (middle) profiles with corresponding RS data (CHAMP-RS) over the U.S. for May 2001-September 2004 ( $\Delta t = 3 h$ ;  $d = 300 km$ ). The right panel shows the number of compared data per altitude (solid line: temperature; dashed line: refractivity).

standard deviations (4.55% former SU, 6.09% China at 10 hPa) compared to the above discussed regions with good agreement. Problems in the RS measurements (Mars/MRZ and Shanghai) are very likely the reason for these deviations. Inaccurate radiation correction [Luers and Eskridge, 1998] or a systematic error in the pressure determination of the RS are possible reasons for these problems.

It is noted, that the GPS RO data at  $\sim 10$  hPa can be influenced by residual errors due to imperfect ionospheric correction applying the bending angle correction by Vorob'ev and Krasil'nikova [1994]. Raytracing simulations using spherical symmetric refractivity distributions by Wickert [2002] indicate that these errors can be on the order of  $\sim 1$  K ( $\sim 0.3\%$  refractivity equivalent) for daytime during maximum of solar activity (SolarMax, worst case). CHAMP measurements during 2001 and 2002 were recorded under SolarMax conditions. However the magnitude of the observed differences between the CHAMP and RS data is larger than this value. Therefore the deviations at 10 hPa are

Region	No. (N)	No. (T)	$\overline{\Delta N}$ [%]	$\sigma_{\Delta N}$ [%]	$\overline{\Delta T}$ [K]	$\sigma_{\Delta T}$ [K]
Australia	112	797	0.35	1.02	-0.35	2.64
China	507	2219	0.16	0.85	-0.45	2.52
Europe	2916	5044	0.13	0.73	-0.27	1.69
Former SU	2297	2695	0.07	0.74	-0.72	1.84
India	1(312)	312	-0.94(0.79)	n.a.(2.09)	-1.63	4.09
Japan	n.a.(586)	586	n.a.(0.22)	n.a.(1.32)	-0.40	2.71
U.S.	5466	5533	0.03	0.88	-0.14	1.87

**Table 4.4:** Comparison of CHAMP refractivity and dry temperature data with RS at 100 hPa over different geographical regions ( $\Delta t = 3 h$ ;  $d = 300 km$ ). n.a. indicates not available humidity data at all. The humidity then was set to 0. above 300 hPa to compare the number of the refractivity data (in brackets) with CHAMP. For details see text.

Region	No. (N)	No. (T)	$\overline{\Delta N}$ [%]	$\sigma_{\Delta N}$ [%]	$\overline{\Delta T}$ [K]	$\sigma_{\Delta T}$ [K]
Australia	134	150	0.44	1.66	-2.05	3.63
China	61	345	-5.60	6.09	2.33	4.96
Europe	823	1755	0.65	1.53	-2.04	3.46
Former SU	259	332	-3.58	4.55	-1.37	3.49
India	n.a.(2)	2	n.a.(-3.82)	n.a.(7.48)	8.95	17.5
Japan	n.a.(381)	381	n.a.(0.75)	n.a.(1.38)	-1.67	3.13
U.S.	4065	4148	-0.51	1.87	-1.00	3.00

**Table 4.5:** Comparison of CHAMP refractivity and dry temperature data with RS at 10 hPa over different geographical regions ( $\Delta t = 3 h$ ;  $d = 300 km$ ). n.a. indicates not available humidity data at all. The humidity then was set to 0. above 300 hPa to compare the number of the refractivity data (in brackets) with CHAMP. For details see text.

probably caused by incorrect RS measurements.

The IM-MK3 RS, used for sounding over India, shows worst results compared to the other geographical regions. Between 500 and 150 hPa these results are still satisfactorily (nearly no refractivity bias in relation to CHAMP, 2 % standard deviation), but above 150 hPa large biases (e.g.,  $\sim 2.5\%$  at 70 hPa or  $-3.82\%$  at 10 hPa) are observed, connected with large standard deviations of  $\sim 3$  and  $7.48\%$ , respectively (see Tabs. 4.4, 4.5 and Fig. 4.13). This indicates serious problems of the used sensors for the IM-MK3 sonde at altitudes above 150 hPa.

The discussion of the comparison results is focused to the refractivity, because it is the independent observable, which is derived from GPS occultation measurements. To derive temperature and water vapor profiles additional assumptions and/or additional meteorological data are necessary (see discussion above). However Figs. 4.10-4.22 indicate, that the dry temperature, derived from the CHAMP RO data can be used above  $\sim 300$  hPa in good approximation as the absolute temperature up to 10 hPa.

Tabs. 4.4 and 4.5 summarize the comparison results at the pressure levels 100 and 10 hPa, respectively. As already discussed above and as can be seen in Figs. 4.10-4.15 the comparison results for different geographical regions are nearly equivalent for some of them, but can be significantly different, depending on the type of the used radio sonde.

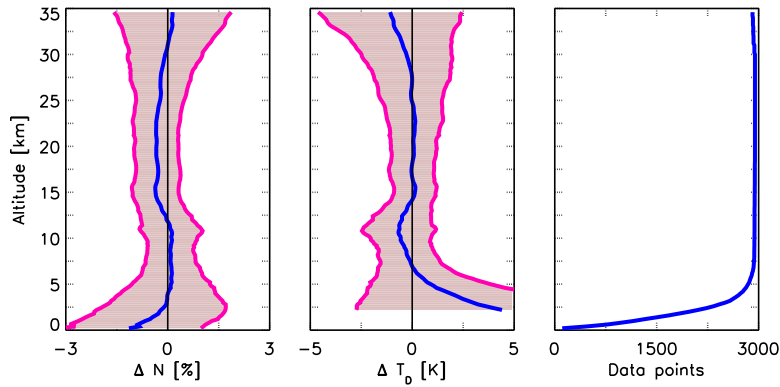


**Figure 4.16:** Comparison (Bias and RMS) of CHAMP refractivity (left panel) and dry temperature (middle) profiles with corresponding ECMWF data (CHAMP-ECMWF) over Europe for May 2001-September 2004 ( $\Delta t = 3 h$ ;  $d = 300 km$ ; 2946 profiles).

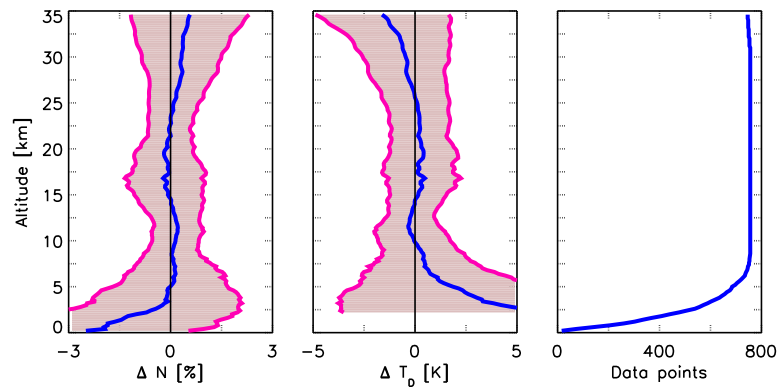


**Figure 4.17:** Comparison (Bias and RMS) of CHAMP refractivity (left panel) and dry temperature (middle) profiles with corresponding ECMWF data (CHAMP-ECMWF) over Australia for May 2001-September 2004 ( $\Delta t = 3 h$ ;  $d = 300 km$ ; 756 profiles).

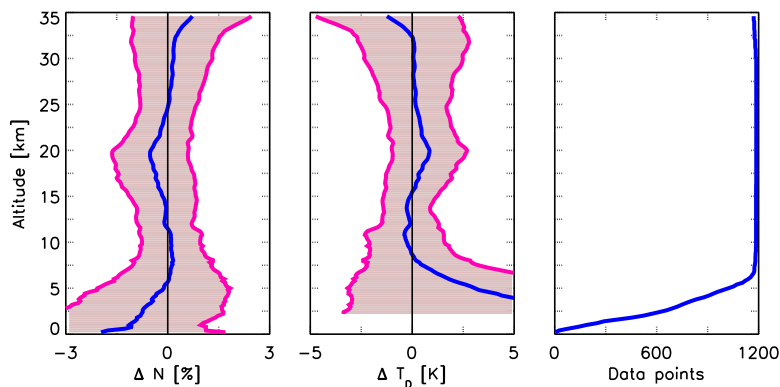


**Figure 4.18:** Comparison (Bias and RMS) of CHAMP refractivity (left panel) and dry temperature (middle) profiles with corresponding ECMWF data (CHAMP-ECMWF) over China for May 2001-September 2004 ( $\Delta t = 3 h$ ;  $d = 300 km$ ; 1186 profiles).

#### 4.2.3 CHAMP vs. ECMWF

The CHAMP profiles for the comparison with the RS data ( $\Delta t=3 h$ ;  $d=300 km$ ), are also compared with meteorological analyzes provided by ECMWF. This is done to ensure that the observed differences in the comparisons with the RS data (Figs. 4.10-4.15) are not caused by different meteorological conditions over the investigated regions.

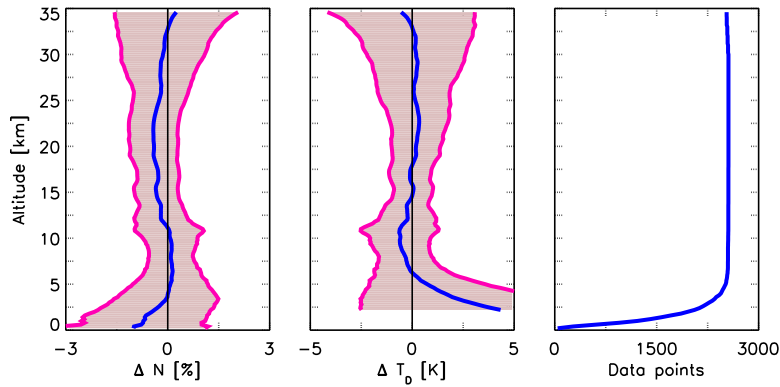


**Figure 4.19:** Comparison (Bias and RMS) of CHAMP refractivity (left panel) and dry temperature (middle) profiles with corresponding ECMWF data (CHAMP-ECMWF) over the countries of the former Soviet Union for May 2001-September 2004 ( $\Delta t = 3 h$ ;  $d = 300 km$ ; 2556 profiles).

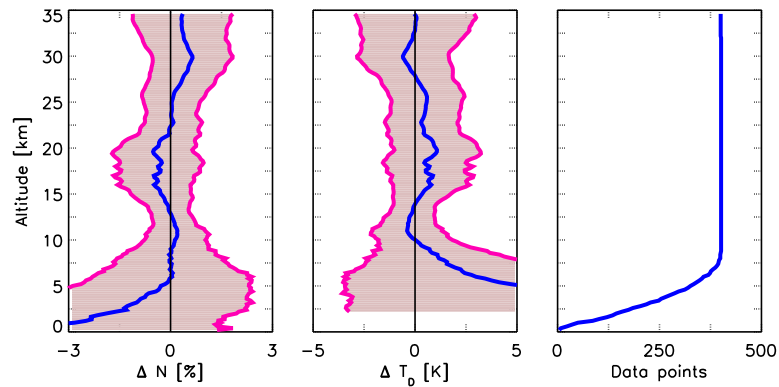


**Figure 4.20:** Comparison (Bias and RMS) of CHAMP refractivity (left panel) and dry temperature (middle) profiles with corresponding ECMWF data (CHAMP-ECMWF) over India for May 2001-September 2004 ( $\Delta t = 3 h$ ;  $d = 300 km$ ; 401 profiles).

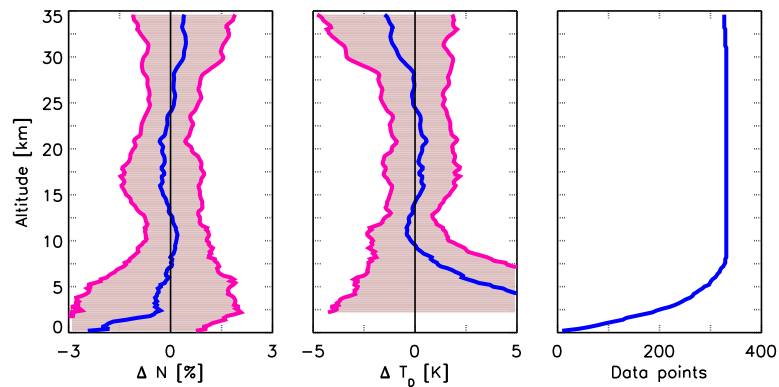


**Figure 4.21:** Comparison (Bias and RMS) of CHAMP refractivity (left panel) and dry temperature (middle) profiles with corresponding ECMWF data (CHAMP-ECMWF) over Japan for May 2001-September 2004 ( $\Delta t = 3 h$ ;  $d = 300 km$ ; 331 profiles).

Linear interpolation in time is performed between the 6 h analyzes fields. Refractivity data are taken from the grid point nearest to the occultation ( $0.5^\circ * 0.5^\circ$  resolution in latitude/longitude, gaussian grid). The maximum distance to this grid point is then  $\sim 20$ - $25 km$  (Equator region). The comparison is performed at the 60 ECMWF model levels ranging from the ground surface up to 0.1 hPa (about 60 km altitude). Vertical spacing of the model grid points increases from about 200 m

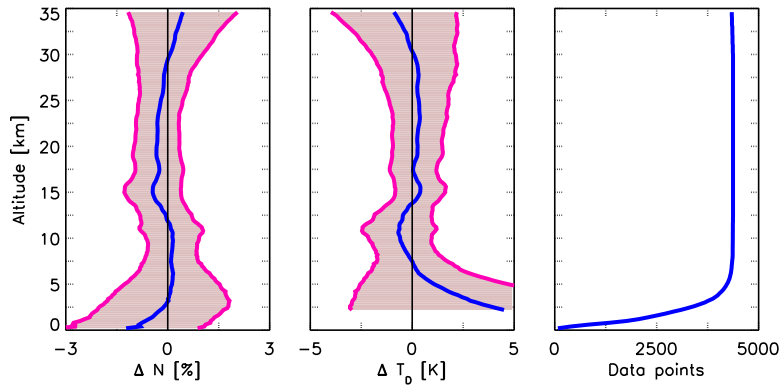


**Figure 4.22:** Comparison (Bias and RMS) of CHAMP refractivity (left panel) and dry temperature (middle) profiles with corresponding ECMWF data (CHAMP-ECMWF) over the U.S. for May 2001-September 2004 ( $\Delta t = 3 h$ ;  $d = 300 km$ ; 4372 profiles).

at 1 km altitude to about 700 m at 10 km. The refractivity from the analysis data was calculated according to Eqn. 4.1. The model data then are interpolated to the 200 m vertical altitude grid of the CHAMP occultation data. The formulas for the calculation of mean and standard deviation of temperature and refractivity are equivalent to Eqns. 4.2-4.5.

In contrast to the radiosonde comparisons (Sec. 4.2.1) the CHAMP data are compared with the analyzes at geometrical altitudes, i.e. the geopotential heights, given for each ECMWF pressure level, are converted to geometrical heights. A second, major, difference in relation to the RS comparisons is the use of dry temperatures not only for the CHAMP data. For that purpose the ECMWF temperatures were converted to ECMWF dry temperatures using the humidity data from the analyzes and the Smith-Weintraub formula (Eqn. 4.1). Since humidity data are available for each ECMWF altitude level, the refractivity always can be calculated and compared with CHAMP data. Consequently the temperature and refractivity comparisons (Figs. 4.16-4.22) are based on the same data pairs, in contrast to the RS comparisons (Fig. 4.10-4.15). The number of compared refractivity and temperature data vs. altitude is indicated in the right panel of the Figs. 4.16-4.22.

Only CHAMP profiles with coinciding RS data were compared with ECMWF, but for each subset (Australia, China, Europe, India, Japan, countries of the former SU and U.S.). The number of compared profiles, is lower than for the RS comparisons (e.g., 2946 vs. 5153 for Europe) since several coincidences with RS measurements may exist for one and the same CHAMP occultation.

The results of the comparisons are shown in Figs. 4.16-4.22. Tab. 4.6 and 4.7 summarize the results at 10 and 30 km, respectively. As expected, the results are very similar. This indicates, that differences, observed in the comparisons with the RS data over different geographical regions (Figs. 4.10-4.15), really can be attributed to the different types of RS. However slightly differences are observed in the comparisons with ECMWF.

At first the general features of Figs. 4.16-4.22 are discussed. Both, refractivity and dry temperature agree very well between  $\sim 5$  and 30 km. Below  $\sim 5$  km a similar negative refractivity bias of the CHAMP measurements in relation to the analyzes is observed as in the RS comparisons (see discussion in Sec. 4.2.1 and 4.2.2). The bias is largest for Australia, India, and Japan with about 1.5% near the Earth's surface. Slightly less values are observed for other regions, e.g., the former SU with  $\sim 1\%$ . The altitude range, where this bias appears, varies with the geographical region. It is  $\sim 5$  km for India and China and less, up to 2.5 km, for the other regions. This is in good agreement with the fact, that the bias is most pronounced in wet regions. More details on the characteristics and

reasons of this refractivity bias are given by *Ao et al.* [2003]; *Beyerle et al.* [2003a, b, 2005].

There is nearly no bias between the CHAMP measurements and the analyzes up to 30 km. Best agreement is observed for Australia (Fig. 4.17). The comparison over India (Fig. 4.20) shows worst results (up to  $\sim -0.6\%$  bias) at these altitudes. A detailed discussion of the deviations is beyond the scope of the study here. Biases can be caused by the RO as well as the analyzes. Above 30 km there is a tendency for a positive bias of the CHAMP data in relation to ECMWF up to  $\sim 0.4\%$  at 35 km for China (Fig. 4.18). The standard deviations fall within the 0.7-1.5% range.

The behavior of the dry temperature deviations corresponds with those of the refractivity. For the lower troposphere a positive bias of the CHAMP dry temperature in relation to ECMWF is observed, which correlates with the negative refractivity bias described above. Above 30 km a slight negative bias (up to  $\sim 1$  K for China or Australia, Figs. 4.18 and 4.17) of the CHAMP data in relation to the analyzes can be observed. Between  $\sim 5$  and 30 km the dry temperature comparisons reveal nearly no bias between CHAMP and ECMWF.

Even though the agreement of the CHAMP data with ECMWF is nearly excellent, slight differences are observed, as discussed above. Tabs. 4.6 and 4.7 give a summary of biases and standard deviations between the RO and analyzes data at 10 and 30 km.

At 10 km (within the altitude region of the highest accuracy of the CHAMP data [*Kursinski et al.*, 1997]) for all investigated regions a slight positive bias of the CHAMP data in relation to ECMWF (0.07-0.17 K) is observed to be very similar for all regions. The standard deviation is less for Australia, Europe and U.S.. At these regions Vaisala RS (at U.S. together with VIZ) data of high quality are used as backbone for the ECMWF data assimilation and probably lead to better quality of

Region	Number	$\overline{\Delta N}[\%]$	$\sigma_{\Delta N}[\%]$	$\overline{\Delta T}[\text{K}]$	$\sigma_{\Delta T}[\text{K}]$
Australia	756	0.14	0.68	-0.05	1.76
China	1186	0.10	0.85	-0.26	1.84
Europe	2946	0.11	0.75	-0.56	1.48
Former SU	2556	0.07	0.80	-0.58	1.48
India	401	0.13	0.90	-0.02	1.81
Japan	331	0.17	0.90	-0.20	1.85
U.S.	4372	0.14	0.78	-0.59	1.55

**Table 4.6:** Comparison of CHAMP refractivity and dry temperature data at 10 km with ECMWF ( $\Delta t = 3$  h;  $d = 300$  km).

Region	Number	$\overline{\Delta N}[\%]$	$\sigma_{\Delta N}[\%]$	$\overline{\Delta T}[\text{K}]$	$\sigma_{\Delta T}[\text{K}]$
Australia	756	0.32	1.16	-0.46	2.10
China	1186	0.17	1.14	-0.06	2.42
Europe	2946	-0.07	1.09	-0.28	2.20
Former SU	2556	-0.14	1.23	0.19	2.41
India	401	0.64	1.18	-0.59	2.24
Japan	331	0.38	1.16	-0.76	2.59
U.S.	4372	0.06	0.96	0.08	2.05

**Table 4.7:** Comparison of CHAMP refractivity and dry temperature data at 30 km with ECMWF ( $\Delta t = 3$  h;  $d = 300$  km).

the analyzes. The dry temperature of CHAMP exhibit a slight cold bias in relation to the analyzes (-0.05..-0.59 K). One possible explanation for this could be the better vertical resolution of the tropopause by the CHAMP data in relation to ECMWF. This leads lead to a cold bias in relation to the analyzes, as first discussed by *Rocken et al.* [1997] for comparisons of GPS/MET occultation measurements with meteorological analyzes from NCEP (National Centers for Environmental Prediction).

The biases between CHAMP and ECMWF data at 30 km exhibit more variability and ranges from -0.14 (former SU) to 0.64% (India), the standard deviation from 0.96 (U.S.) to 1.23% (former SU). The dry temperature bias ranges from -0.76 to 0.19 K, the standard deviation from 2.05 to 2.59 K (see Tab. 4.7).

To discuss and interpret the comparison results at these altitudes more detailed investigations are needed, which are beyond the scope of this study. At these altitudes the accuracy of the analyzes is less accurate compared to lower altitudes, but also the error potential of the GPS measurements is higher as, e.g., at 10 km [*Kursinski et al.*, 1997].

## 5 Summary and conclusions

GPS radio occultation measurements from the German CHAMP satellite between 2001 and 2004 were compared with radiosonde data and meteorological analyzes from ECMWF. A set of 162,461 vertical refractivity and dry temperature profiles from CHAMP was used for this study.

For occultations over Europe (Vaisala radiosondes) the maximum distance  $d$  and maximum time difference  $\Delta t$  between RS and RO measurement was varied from 100 to 300 km and 1 to 3 h, respectively. It was shown that the resulting bias is practically independent of the used combination of  $d$  and  $\Delta t$ . In contrast the standard deviation is lowest for  $d = 100 \text{ km}$  with  $\sim 0.5\%$  and increases to  $\sim 0.7\%$  for  $d = 300 \text{ km}$ . The variation of  $d$  is more significant to the comparison results, rather than variation of  $\Delta t$ . The bias between CHAMP and RS measurements is practically not influenced by the various combinations of  $d$  and  $\Delta t$ . For that reason a combination  $\Delta t = 3 \text{ h}$  and  $d = 300 \text{ km}$  was used for the subsequent investigations to get more statistical confidence by using more extensive data sets for the comparisons.

CHAMP and RS data were compared over different geographical regions (Australia, China, Europe, countries of the former SU, India, Japan, and U.S.), where different types of radiosondes are in use. The results of these investigations show similarities, but also significant differences, depending on the RS type used for the according comparison. The, in part considerable, lack of relative humidity data in the higher troposphere and at altitudes above, indicates serious problems in the water vapor measurements of the radiosondes.

Best agreement with CHAMP between 500 and 10 hPa level is observed over Australia, Europe, Japan and U.S. (Vaisala, VIZ, Meisei) with nearly no bias and standard deviations less than 1% at 100 hPa and  $\sim 1.5\%$  at 10 hPa. Nearly perfect is the agreement over U.S. (VIZ/Vaisala) at these altitudes, e.g., at 100 hPa a bias of 0.03% is observed. The slightly higher bias over Australia (e.g., 0.35% at 100 hPa) or Europe (e.g., 0.13% at 100 hPa) is probably related to incorrect water vapor measurements of the RS.

Less perfect agreement is observed for China (Shanghai RS) and the countries of the former SU (Mars/MRZ RS). Up to pressure levels of  $\sim 40 \text{ hPa}$  the comparison results are comparable to those of, e.g., Europe or U.S., however at upper altitudes large biases are observed (-3.58% former SU, -5.60% China at 10 hPa) which are connected with higher standard deviations (4.55% former SU,

6.09% China at 10 hPa). This is related to possible problems in the radiation correction and/or significant imperfect pressure measurements at these altitudes for Mars/MRZ and Shanghai RS, respectively.

The comparison of the CHAMP data with the Indian IM-MK3 radiosonde shows worst results of the study. Above 150 hPa significant larger biases and standard deviations compared to other regions are observed, indicating serious problems of the IM-MK3 radiosonde at these altitudes.

In general at the upper altitudes (e.g., at 10 hPa), also for the regions with better agreement between RS and CHAMP RO, the accordance between the different regions is slightly worse and the deviations show different behavior (e.g., bias for U.S. -0.51%, for Europe +0.65%). This is also related to the RS data, rather than the CHAMP measurements, but must be investigated in more detail within future studies.

The discussion of the comparison results is focused to the refractivity, because it is the independent observable, which is derived from GPS occultation measurements. Additional assumptions and/or additional meteorological data are necessary to derive temperature and water vapor profiles. However it was shown, that the dry temperature, derived from the CHAMP RO data can be used above  $\sim 300$  hPa in good approximation as the absolute (“wet“) temperature up to 10 hPa.

The subsets of CHAMP measurements over the different geographical regions were also compared with ECMWF to verify the RS results. The deviations, found in these comparisons, are very similar for every investigated region. This indicates that the observed differences in the radiosonde comparisons are caused by the various types of the used RS and not by different meteorological conditions over the investigated regions.

This study is an initial investigation of several aspects when comparing RS data with CHAMP occultations. It is planned to extend this kind of studies and to investigate in more detail, e.g., the deviations, observed at higher altitudes, e.g., at  $\sim 10$  hPa.

In general it can be concluded that GPS radio occultation data from CHAMP are a valuable source to reveal weaknesses of radiosonde measurements.

## Acknowledgements

This study is result of the routine work on the CHAMP data and also result of a visiting scientist activity of the GRAS (GNSS Receiver for Atmosphere Sounding) SAF (Satellite Application Facility), which is hosted by the Danish Meteorological Institute (DMI) at Copenhagen and funded by EUMETSAT. I thank Georg Larsen, Kent Lauritsen, Frans Rubek and Martin Sørensen for the great hospitality and the unique chance to work for a month together with them. Radiosonde data were made available by the Freie Universität Berlin by Kathrin Schöllhammer. Bill Kuo provided Fig. 2.1. ECMWF analysis data were provided by the Deutscher Wetterdienst. My institute and Prof. Christoph Reiger, the Principal Investigator of the CHAMP mission, supported the stay at DMI. Without the work of Torsten Schmidt, Georg Beyerle, Stefan Heise and other colleagues at GFZ such investigations, as performed within this study, would not have been possible. I thank all of them.

## References

Ao, C. O., T. K. Meehan, G. A. Hajj, A. J. Mannucci, and G. Beyerle, Lower-troposphere refractivity bias in GPS occultation retrievals, *J. Geophys. Res.*, 108(D18), doi:10.1029/2002JD003,216, 2003.

- Beyerle, G., M. E. Gorbunov, and C. O. Ao, Simulation studies of GPS radio occultation measurements, *Radio Sci.*, 38(5), doi:10.1029/2002RS002,800, 2003a.
- Beyerle, G., J. Wickert, T. Schmidt, and C. Reigber, Atmospheric sounding by GNSS radio occultation: An analysis of the negative refractivity bias using CHAMP observations, *J. Geophys. Res.*, p. doi:10.1029/2003JD003922, 2003b.
- Beyerle, G., T. Schmidt, J. Wickert, S. Heise, and C. Reigber, An analysis of refractivity biases detected in GPS radio occultation data: Results from simulation studies, aerological soundings and CHAMP satellite observations, *J. Geophys. Res.*, subm., 2005.
- Deutscher Wetterdienst, Verzeichnis der Meldestellen des synoptischen Dienstes, Stand 09.01.1996, (in German), *Vorschriften und Betriebsunterlagen des DWD, Nr. 1, Offenbach*, 1996.
- Dzingel, M., and U. Leiterer, Untersuchungen über Genauigkeit und Korrekturmöglichkeiten für die Feuchtesondierung mit dem A-Humicap der Sonde RS-80, *Technical Report, Meteorologisches Observatorium Lindenberg*, 1995.
- Elliot, W. P., and D. Gaffen, On the utility of radiosonde humidity archives for climate change studies, *Bull. Amer. Meteor. Soc.*, (72), 1507–1520, 1991.
- Foelsche, U., G. Kirchengast, A. Gobiet, A. Steiner, A. Löscher, J. Wickert, and T. Schmidt, The CHAMPCLIM project: An overview, in *Earth Observation with CHAMP: Results from Three Years in Orbit*, edited by C. Reigber, P. Schwintzer, H. Lühr, and J. Wickert, pp. 615–620, Springer Verlag, 2005.
- Gorbunov, M. E., and S. Sokolovskiy, Remote sensing of refractivity from space for global observations of atmospheric parameters, *Rep. 119, Max Planck-Inst. for Meteorol., Hamburg*, 1993.
- Hajj, G. A., E. R. Kursinski, L. J. Romans, W. I. Bertiger, and S. S. Leroy, A technical description of atmospheric sounding by GPS occultation, *J. Atmos. Solar-Terr. Phys.*, 64(4), 451–469, 2002.
- Hajj, G. A., et al., CHAMP and SAC-C atmospheric occultation results and intercomparisons, *J. Geophys. Res.*, 109, doi:10.1029/2003JD003909, 2004.
- Healy, S., and J. Eyre, Retrieving temperature, water vapor and surface pressure information from refractive-index profiles derived by radio occultation: A simulation study, *Quart. J. Roy. Meteorol. Soc.*, 126, 1661–1683, 2000.
- Healy, S., A. Jupp, and C. Marquardt, Forecast impact experiments with CHAMP GPS radio occultation measurements: Preliminary results, *Geophys. Res. Lett.*, in print, 2005.
- Hedin, A. E., Extension of the MSIS thermosphere model into the middle and lower atmosphere, *J. Geophys. Res.*, 96, 1159–1172, 1991.
- Heise, S., J. Wickert, G. Beyerle, T. Schmidt, and C. Reigber, Global monitoring of tropospheric water vapor with GPS radio occultation aboard CHAMP, *Adv. Space Res.*, subm., 2005.
- Jakowski, N., A. Wehrenpfennig, S. Heise, C. Reigber, H. Lühr, L. Grunwaldt, and T. K. Meehan, GPS radio occultation measurements of the ionosphere from CHAMP: Early results, *Geophys. Res. Lett.*, 29(10), doi:10.1029/2002RS002763, 2002.
- Jensen, A. S., M. Lohmann, H.-H. Benzon, and A. Nielsen, Full spectrum inversion of radio occultation signals, *Radio Sci.*, 38(3), doi:10.1029/2002RS002763, 2003.

- Kraus, H., *Die Atmosphäre der Erde: Eine Einführung in die Meteorologie (in German)*, Springer Verlag, 2001.
- Kuo, Y.-H., T.-K. Wee, S. Sokolovskiy, C. Rocken, W. Schreiner, D. Hunt, and R. A. Anthes, Inversion and error estimation of GPS radio occultation data, *J. Meteorol. Soc. Jpn.*, 1B(82), 507–531, 2004.
- Kuo, Y.-H., W. S. Schreiner, J. Wang, D. L. Rossiter, and Y. Zhang, Comparison of GPS Radio occultation soundings with radiosondes, *Geophys. Res. Lett.*, subm., 2005.
- Kursinski, E. R., G. A. Hajj, J. T. Schofield, R. P. Linfield, and K. R. Hardy, Observing Earth's atmosphere with radio occultation measurements using Global Positioning System, *J. Geophys. Res.*, 19(D19), 23,429–23,465, 1997.
- Kursinski, E. R., et al., Initial results of radio occultation observations of Earth's atmosphere using the Global Positioning System, *Science*, 271, 1107–1110, 1996.
- Larsen, G., K. Lauritsen, F. Rubek, and M. Sørensen, Processing of CHAMP radio occultation data using GRAS SAF software, in *Earth Observation with CHAMP: Results from Three Years in Orbit*, edited by C. Reigber, P. Schwintzer, H. Lühr, and J. Wickert, pp. 543–548, Springer Verlag, 2005.
- Leiterer, U., H. Dier, and T. Naebert, Improvements in Radiosonde Humidity Profiles using RS 80/RS90 Radiosondes of Vaisala, *Beitr. Phys. Atmosph.*, 4(70), 1997.
- Loiselet, M., N. Stricker, Y. Menard, and J. Luntama, GRAS – MetOps GPS based atmospheric sounder, *ESA Bulletin*, May, 102, 38–44, 2000.
- Luers, J. K., and R. E. Eskridge, Use of radiosonde temperature data in climate studies, *J. Climate*, 11, 1002–1019, 1998.
- Marquardt, C., K. Schöllhammer, G. Beyerle, T. Schmidt, J. Wickert, and C. Reigber, Validation and data quality of CHAMP radio occultation data, in *First CHAMP Mission Results for Gravity, Magnetic and Atmospheric Studies*, pp. 384–396, Springer Verlag, 2003.
- Ratnam, M. V., T. Tsuda, C. Jacobi, and Y. Aoyama, Enhancement of gravity wave activity observed during a major southern hemisphere stratospheric warming by CHAMP/GPS measurements, *Geophys. Res. Lett.*, 31(L16101), doi:10.1029/2004GL019789, 2004.
- Reigber, C., P. Schwintzer, H. Lühr, and J. Wickert (Eds.), *Earth Observation with CHAMP: Results from Three Years in Orbit*, Springer Verlag, 2005.
- Rocken, C., Y.-H. Kuo, W. Schreiner, D. Hunt, S. Sokolovskiy, and C. McCormick, COSMIC system description, *Terrestrial, Atmospheric and Oceanic Sciences*, 11, 21–52, 2000.
- Rocken, C., et al., Analysis and validation of GPS/MET data in the neutral atmosphere, *J. Geophys. Res.*, 102(D25), 29,849–29,866, 1997.
- Schmidt, T., J. Wickert, G. Beyerle, and C. Reigber, Tropical tropopause parameters derived from GPS radio occultation measurements with CHAMP, *J. Geophys. Res.*, 109(D13105), doi:10.1029/2004JD004566, 2004.
- Schmidt, T., J. Wickert, G. Beyerle, R. König, R. Galas, and C. Reigber, The CHAMP atmospheric processing system for Radio occultation measurements, in *Earth Observation with CHAMP: Results from Three Years in Orbit*, edited by C. Reigber, P. Schwintzer, H. Lühr, and J. Wickert, Springer Verlag, 2005.

- Seidel, D. J., R. J. Ross, J. K. Angell, and G. C. Reid, Climatological characteristics of the tropical tropopause as revealed by radiosondes, *J. Geophys. Res.*, 106, 7857–7878, 2001.
- Smith, E., and S. Weintraub, The constants in the equation for atmospheric refractive index at radio frequencies, *Proc. IEEE*, 41, 1953.
- Soden, B. J., and J. R. Lanzante, An assessment of satellite and radiosonde climatologies of upper-tropospheric water vapor, *J. Climate*, 9, 1235–1250, 1995.
- Sokolovskiy, S. V., Tracking tropospheric radio occultation signals from low Earth orbit, *Radio Sci.*, 36(3), 483–498, 2001.
- Sokolovskiy, S. V., and D. C. Hunt, Statistical optimization approach for GPS/MET data inversion, *URSI GPS/MET workshop, Union Radio Sci. Int.*, 1996.
- Vaisala, *Users guide ozone sonde OES*, pp. Vaisala Oy, Helsinki, 1991.
- Vorob'ev, V. V., and T. G. Krasil'nikova, Estimation of the accuracy of the refractive index recovery from Doppler shift measurements at frequencies used in the NAVSTAR system, *Phys. Atmos. Ocean*, 29, 602–609, 1994.
- Wang, D. Y., et al., Cross-validation of MIPAS/ENVISAT and GPS-RO/CHAMP temperature profiles, *J. Geophys. Res.*, 109, doi:10.1029/2004JD004963, 2004.
- Ware, R., et al., GPS sounding of the atmosphere from low Earth orbit: Preliminary results, *Bull. Am. Meteorol. Soc.*, 77(1), 19–40, 1996.
- Wickert, J., The CHAMP radio occultation experiment: Algorithms, Processing system, and First results (in German), *Scientific Technical Report 02/07*, 2002.
- Wickert, J., R. Galas, G. Beyerle, R. König, and C. Reigber, GPS ground station data for CHAMP radio occultation measurements, *Phys. Chem. Earth (A)*, 26, 2001a.
- Wickert, J., C. Ao, and W. Schreiner, GPS radio occultation with CHAMP: Comparison and evaluation of data analysis from GFZ, JPL and UCAR, *EGU 1. General Assembly, Nice, France, April 2004*, abstract EGU04-A-02805, 2004a.
- Wickert, J., A. Pavelyev, Y. A. Liou, T. Schmidt, C. Reigber, A. Pavelyev, K. Igarashi, and S. Matyugov, Amplitude variations in the GPS signals as a possible indicator of the ionospheric structures, *Geophys. Res. Lett.*, 31, 124801, doi:10.1029/2004GL020607, 2004b.
- Wickert, J., T. Schmidt, G. Beyerle, R. König, C. Reigber, and N. Jakowski, The radio occultation experiment aboard CHAMP: Operational data processing and validation of atmospheric parameters, *J. Meteorol. Soc. Jpn.*, 82(1B), 381–395, 2004c.
- Wickert, J., G. Beyerle, R. König, S. Heise, L. Grunwaldt, G. Michalak, C. Reigber, and T. Schmidt, GPS radio occultation with CHAMP and GRACE: A first look at a new and promising satellite configuration for global atmospheric sounding, *Ann. Geophysicae*, in print, 2005a.
- Wickert, J., T. Schmidt, G. Beyerle, G. Michalak, R. König, S. Heise, and C. Reigber, GPS radio occultation with CHAMP and GRACE: Recent results, in *Proc. OPAC-2 workshop, Graz September 2004*, edited by G. Kirchengast, U. Foelsche, and A. K. Steiner, Springer Verlag, 2005b.
- Wickert, J., et al., Atmosphere sounding by GPS radio occultation: First results from CHAMP, *Geophys. Res. Lett.*, 28(17), 3263–3266, 2001b.